REPUBLIC OF TURKEY
ALTINBAŞ UNIVERSITY
Institute of Graduate Studies

Electrical and Computer Engineering

COMPUTER AIDED DIAGNOSIS OF BREAST TUMOR SEGMENTATION AND CLASSIFICATION ON CT IMAGES USING MACHINE LEARNING

Barish Mohammed IZADDIN IZADDIN

Master of Science

Supervisor
Asst. Prof. Dr. Ayça Kurnaz TÜRKBEN

Istanbul, 2021

COMPUTER AIDED DIAGNOSIS OF BREAST TUMOR SEGMENTATION AND CLASSIFICATION ON CT IMAGES USING MACHINE LEARNING

by

Barish Mohanmmed Izaddin Izaddin

Electrical and Computer Engineering

Master of Science

ALTINBAŞ UNIVERSITY

2021

The thesis titled “COMPUTER AIDED DIAGNOSIS of BREAST TUMOR SEGMENTATION AND CLASSIFICATION ON CT IMAGES USING MACHINE LEARNING ” prepared and presented by “ Barish Mohammed IZADDIN IZADDIN ” was accepted as a Master of Science Thesis inElectrical and Computer Engineering.

____

Asst. Prof. Dr. Ayça Kurnaz TÜRKBEN

Supervisor

Thesis Defense Jury Members:

Asst. Prof. Ayça Kurnaz TÜRBEN	School of Engineering and Architecture, Altinbas University	______________________
Asst. Prof. Dr. Abdullahi Abdu IBRAHIM	School of Engineering and Architecture, Altinbas University	______________________
Asst. Prof. Dr. Tarik Abed MOHAMMED	Electrical and computer Engineering Department Imm Jaafar AL-sadiq University	______________________

I certify that this thesis satisfies all the requirements as a thesis for the degree of Master of Science.

Approval Date of Institute of Graduate Studies:

____/____/____

I hereby declare that all information/data presented in this graduation project has been obtained in full accordance with academic rules and ethical conduct. I also declare all unoriginal materials and conclusions have been cited in the text and all references mentioned in the Reference List have been cited in the text, and vice versa as required by the abovementioned rules and conduct.

Barish Mohammed Izadddin Izaddin

ABSTRACT

COMPUTER AIDED DIAGNOSIS of BREAST TUMOR SEGMENTATION AND CLASSIFICATION ON CT IMAGES USING MACHINE LEARNING

Izaddin Izaddin,Mohammed Barish

M.Sc., Electrical and Computer Engineering, Altınbaş University,

Supervisor:. Ass. Prof. Dr. Ayça Kurnaz Türkben

Date: 2021

Pages: 41

Computed tomography and Mammography are a screening procedure for early identification of breast tumor symptoms such as masses, calcifications, bilateral asymmetry, and architectural deformation. Because human observers are limited, computers play a critical role in identifying early indications of cancer. The vast range of characteristics that identify abnormalities, as well as the fact that they are frequently indistinguishable from surrounding tissue, make computer-aided breast abnormality detection difficult. This thesis investigates how to use well-known image processing and machine learning techniques to help breast tumor diagnosis using: computed tomography images and Mammography. Therefore, this research aims to develop a computer-aided breast tumor screening technique (segmentation and classification) based on mammography images that aid pathologists in their decision-making. Using machine learning methods based on neural networks and logistic regression, a real application is created and constructed, which includes both initial picture processing and subsequent cancer diagnosis. The app is tested on a set of mammography pictures, and the results are displayed and explained in depth. The utilization of a mix of neural networks and logistic regression in breast cancer diagnosis, as well as real breast tumor images (with different location and size of tumors) acquired in collaboration with the Kirkuk Hospital cancer center, distinguishes this thesis.

Keyword : Brest Tumor, Image processing neural Network , Fuzzy c-Means and Thresholding (FCMT)

TABLE OF CONTENTS

Pages

LIST OF FIGURES

Pages

LIST OF TABLES

<u>Pages</u>

LIST OF ABBREVIATIONS

CT	:	Computed Tomography
CXR	:	Chest X-Ray
MRI	:	Magnetic Resonance Imaging
CAD	:	Computer-Assisted Diagnosis
PNN	:	Probabilistic Neural Network
FCM	:	Fuzzy Clustering Means
FP	:	False-Positive Cases7
DDSM	:	Digital Database For Screening Mammography
MIAS	:	Mammographic Image Analysis Society
CBIS	:	Curated Breast Imaging Subset
ROIs	:	Regions Of Interest
WDMR	:	Wavelet Decomposition And Multi-Scale Region-Growing
DSSM	:	Double-Strategy Splitting Model
CSS	:	Curvature Scale Space
SVM	:	Support Vector Machine
CAGA	:	Chain-Like Agent Genetic Algorithm
FCNN	:	Fast Scanning Deep Convolutional Neural Network
ML	:	Machine Learning
HOG	:	Histogram of Oriented Gradient
BCDR	:	Breast Cancer Digital Repository
DFO	:	Dragon Fly Optimization
FFNN	:	Feed Forward Neural Network
CBET	:	Contrast Balance Enhancement Technique
CLAHE	:	Contrast Limited Adaptive Histogram Equalization
GLCM	:	Gray Level Interaction Matrix

DWT	:	Discrete Wavelet Transform
PPNN	:	Parzen Probabilistic Neural Network
PDF	:	Probability Density Function
DDSM	:	Digital Database for Screening Mammography
SSIM	:	Structured Similarity Index
MSE	:	Mean Square Error
PSNR	:	Peak Signal-To-Noise Ratio
PCD	:	Pixel Detected Percentage
PND	:	Pixel Not Detected Percentage
PFA	:	False Positive Rate
MS	:	Merit Score
TP	:	True Positive
TN	:	True Negative
FN	:	False Positive
IoU	:	Intersection Over Union
DSC	:	Dice Similarity Coeffcient

1. INTRODUCTION

The relevance of the work. In the areas of modern medicine, a new area of processing and analysis of visual data is actively developing - radiomics - computer technology that allows for a deeper analysis of medical images. For example, computed tomography (CT), Magnetic Resonance Imaging (MRI), and chest x-ray (CXR) [1, 2, 3, 4].

This approach allows extracting quantitative textural features from images and isolating biological markers to describe pathology (tumor), which provides a personalized approach to diagnosis and treatment [5, 6, 7, 8, 9]. Development of information technologies - spectral decomposition and neural networks for processing and analyzing visual data are a priority approach for solving this kind of applied problems [10, 11, 12, 13].

At the same time, in the process of recognizing images when making decisions, medical specialists face a number of problems: incomplete and inaccurate initial information; high variability of attributes and small sample sizes; limited decision-making time for conclusions [14, 8, 15, 16, 17]. These factors often lead to diagnostic errors. To enhance the efficiency and qualities of experimental information processing, it is necessary to improve and modify the methods for analyzing visual data, both to improve the quality of medical images and to increase the accuracy of object recognition.

The main advantages of computer vision is to interpret the surrounding space (scene). Methods of segmentation, boundary detection and pattern recognition play an important role, since they are used as the main stage of data processing in most tasks of computer vision and computer diagnostics [16, 18, 19].

This direction covers almost all areas related to medical experimental research. In theoretical terms, pattern recognition can be distinguished into a separate class of tasks related to segmentation and recognition of three-dimensional visual objects, while segmentation is one of the stages of the object recognition task [20, 21].

In the last decade, hardware support in experimental medical research has been actively developing, more and more sophisticated and complex instrumental systems appear. At the same time, the known algorithmic tools do not fully meet the requirements for the speed and quality of processing complex visual data recorded by newly created hardware, as well as the possibilities for solving new urgent problems of geometric (morphological, texture) data analysis based on wavelet and shiarlet data. transformations [22, 23].

1.1. PROBLEM STATEMENT

Breast cancer is a devastating worldwide disease that afflicts millions of women. It is possible to save lives by detecting this cancer in its early stages. Furthermore, it is well known that the most and common method for diagnosing cancer in its early stages is mammography.

Radiologists can anticipate if a mammogram will be accurate more than 90% of the time. Despite this, radiologists are likely to overlook 10% to 15% of breast cancer cases (Erickson, 2005). By double-checking and interpreting mammography pictures, the risk of a false positive can be minimized. Double-checking necessitates the examination of the same mammography by two separate radiologists at different times. Although the accuracy of accurate detection can be enhanced by 15% when compared to single checking. Nevertheless, this operation is costly and taking a long time for performance. The Computer-Assisted Diagnosis (CAD) and Computer-Aided Diagnosis Detection (CADD) can minimize this expense in use. That example, a computer system may be utilized to diagnose medical conditions. Database, image processing, machine learning, and data analysis are among the tools and techniques used in this diagnostic. The question is how these technologies can be used to minimize the object false detection in the mammography breast cancer screening procedure. The use of machine learning, segmentation, classification, and image preprocessing are more potential approach.

Here, machine learning and image processing are implemented to help in identifying breast cancer in mammography pictures. Many image processing algorithms are used to process mammography pictures, starting with noise reduction filters and finishing with feature extraction, edge detection, and region of interest to identify masses. The characteristics retrieved from the processed pictures are then used in the comparison and detection procedures. The accuracy of these systems, on the other hand, is debatable.

To solve new problems, the computational technology of geometric (morphological, texture) analysis of visual data must be modified by allowing users to select machine learning algorithms as a probabilistic neural network (PNN), which will improve the accuracy of linear structure selection, as well as the visual quality of images studied objects and their contours [24, 25, 26,27, 28, 29].

Theoretical and applied research on the improvement of algorithms associated with the use of neural networks within the framework of a unified computational technology for solving problems of assessing the state of an object (identifying and classifying pathologies and neoplasms) on medical images (CXR-scanning, CT and MRI images) is also relevant [8, 30, 31, 75].

1.1.1. MRI of The Breast

Magnetic Resonance Imaging (MRI) seems to be the most appealing option to mammography for detecting some tumors that may be overlooked by experts and determining how to treat women having BT by determining the disease stage.

1.1.2. Breast Cancer Diagnosis

The screening procedure is used to detect breast cancer. This approach involves a doctor or nurse performing a physical examination to look for malignancies. Mammography and other imaging modalities are also used as screening tools. Cancer can be detected in its early stages thanks to screening. Mammography is the greatest approach for early diagnosis analysis and detection of breast tumor to classify since it is easy, affordable, and quick. The identification of anomalies in mammography, such as masses and calcifications, is the first step in detecting breast cancer. Furthermore, numerous minor indications can be recognized. The detection rate of radiography for breast cancer has been reported to be 76 percent to 94 percent, which is much more than 50 percent greater than conventional clinical examinations [32].

1.2. OBJECTIVE OF THIS WORK

This dissertation proposes a method for identifying breast cancer in mammography pictures. The method is divided into two sections. Image processing methods are employed in the initial phase to prepare images for pattern and feature extraction operations. The collected characteristics are sent into a machine learning method that includes a logistic regression and neural network. As a supervised method, input pictures must be used to train it.

The main goals of the project may be stated as follows:

1- Detecting breast cancer by implementing a new CAD system.
2- 2- In the novel suggested approach, image processing methods and supervised machine learning are used.
3- Improving the accuracy of algorithms for segmentation and object recognition in images for visualization and interpretation of experimental medical data.
4- 4- Reducing the likelihood of a false positive in the breast cancer diagnosis procedure.

To achieve the goal, the following tasks have been set:

1. Develop and research a method for segmentation of local areas (with pathology) on medical images (MRI and CT).

2. To develop and research a fast algorithm for the classification of local areas in complex diagnostics (example of malignant and intimate tumor of the breast).

3. Develop and research a high-precision method for detecting the boundaries of objects based on a modified segmentation method.

Conduct experimental studies to assess the advantages of the developed system, algorithms in the framework of a comprehensive medical experiment.

The research methods are to solve the problems posed in the work, the methods of the theory of digital image processing, information theory, methods of the theory of pattern recognition and data analysis, methods of object-oriented programming were used.

1.3. ORGANIZATION OF THESIS

As mentioned earlier, that is dissertation reviews and analyzes the neural networks for breast tumor classification and segmentation. Additionally, the performance of methods is evaluated and compared with the dataset. In Chapter 2, the literature review and theoretical background are investigated. The research questions and research methodologies of this dissertation are explained in Chapter 3. Additionally, some literature and experiments are reviewed. Chapter 4 discusses the experiments and results. Conclusions and some future directions are then drawn in Chapter 5

2. THEORETICAL BACKGROUND AND LITERATURE REVIEW

2.1. THE ROCESSING AND ANALYZING METHODS

Researchers have made several attempts to enhance the diagnostic effectiveness of breast cancer detection by employing fuzzy logic, evolutionary computing, and artificial neural.

Clinics mostly use digital technology to confirm and emphasize decision-making in their experiments. Diagnostic results are usually based on a medical image, which medical practitioners often utilize to recognize patients' problems. Doctors develop an appropriate treatment plan according to the obtained information of the image (especially the object's boundaries). However, inaccuracy in the diagnosis occurs due to lacking image information (because of the ineffective processing)

Therefore, for accurate diagnostics, it is necessary to obtain more information using computational technologies. Edge detection and pattern recognition are essential tools in the image processing field, especially in detecting and extracting objects of interest. The main goal of these methods is to identify the digital image's points on which the image depends [11].

There are numerous studies in this subject area [33, 34], as example the use of MRI [35], extraction of areas of white breast tissue and unicellular detection [36], topological visualization of human breast proliferation using MRI [37]. It is known that fractionation is a necessary but difficult step in classifying and analyzing medical imaging data.

Removing a local object (breast tumor) requires dividing the MRI images into two areas [38]. One area contains a local studied object (breast tumor cells), the second area contains normal cells [5]. Fuzzy clustering tools (FCM), which are often used for image segmentation, were proposed in [39]. In [40], a method of dividing into two regions (breast tumor) based on a hybrid approach was proposed.

In this task, the similarity rate for measuring segmented gray and white matter based on MRI images is considered an important characteristic. The distribution of linear and nonlinear features (edges, boundaries, object attributes) (methods such as

Canny, Pruitt, Log, Roberts, and Pruitt [41, 42], and shift transformation [43]) can be used in solving issues in image analysis.

Modern methods of identification and assessment of local areas (tumors) are subdivided into spatial and contour. Spatial methods [44, 45, 76] define groups of pixels that have some similarities. These methods free the radiologist from some computational operations by automating some features of low-level operations (e.g., graph analysis, classification, and threshold selection).

It is known that early detection of a tumor (e.g., breast) followed by appropriate treatment can reduce the risks [46]. The awareness that this tumor is a type of oncological tumor plays an important role in making doctors' decisions on the use of adequate treatment methods and, thus, on the restoration of human health [47, 48].

According to [49], determining the type of tumor is a difficult task. The main reason is isolated ducts with a poorly defined mass, some characteristics of tumors are clustered, etc., are not well identified due to low contrast and ambiguity of tumor boundaries on ultrasound images.

In [50], the authors proposed a new computational basis for identifying and segmenting objects (breast tumor) in ultrasound images. In [36], a method is proposed that includes the detection of a local object (breast tumor) by segmentation of mammography images (using simple techniques of image processing) that give accepted outcomes in real-time.

Practically, the methods (wavelet transform and the K-clustering method) are implemented to segment an oncological tumor on mammographic images [51]. Then, the K-mean algorithm is used to the contrasted image, in which the tumor area can be detected by thresholding.

A double cut-off approach for enhancing mammography image segmentation was applied in [52]. As an outline to the original image, borders were added to the final segmented image to help doctors identify breast tumors on different quality mammograms.

Detecting breast tumors on mammograms using a convolutional neural network will aid doctors in giving an accurate diagnose of the disease. Deep learning (e.g., neural networks) is a method used to classify objects of interest (abnormal and normal) to solve a diagnostic problem [53, 54].

This need for conclusion and diagnosis, including the simultaneous consideration of information from different sources, is a prerequisite for the detailed analysis of medical images. In the dissertation, various automatic analysis methods of the obtained images of objects of interest (breast tumors) are considered.

In [55], the authors proposed a methodology digitized histopathology images to automate the detecting and segmenting of interest structures. The image information in the proposed method is integrated into three levels for preprocessing the pixel values belog to a region of inerest and relationships with pixels to perform the identify object boundaries, segmentation and classification [55].

Current research demonstrates the utility of nuclear segmentation algorithm and or glandular extraction accurately of different nuclear features and morphological for automated grading of:

1. Breast cancer.
2. Prostate cancer.
3. Recognizing and differentiating between benign and cancerous breast histology specimens.

In [56], the authors proposed a novel breast ROI extraction approach. The approach aims to minimize false-positive cases (FP) based on the neural network and local pixel information. Additionally, the model consists of two stages:

1. Training: A trained model is built in the training stage, where the number of features are extracted from both detected object.
2. Testing: To detect or segment the object from the background, this stage involves image scan.

Afterward, the model used to identify the region of interest and take off background of non infected area. Lastly, the authors used their experiments on an on-dataset of 250 CT images (100 malignant and 150 benign).

A set of computational tools was presented in [57] to aid in detecting and segmenting mammograms that consisted of mass or masses in the views of MLO and CC. In the beginning, an artifact removal algorithm is used. Then, image denoising and gray-level enhancement method based on the Wiener filter and wavelet transform. Lastly, the authors employed a method for detecting and segmentation masses using genetic algorithm, wavelet transform, and multiple thresholding in mammograms. It is worth mentioning that Digital Database for Screening Mammography (DDSM) is used to choose mammograms randomly.

An easy and simple approach introduced in [58] can detect and segment the tumor to classify it with high accuracy in the mammogram images.

The [59] proposes to use the retrieved categorization feature extraction methods on mammography contours in their study (determined by segmentation methods). The procedures are used to categorize mammography tumors based on their diagnosis (malignant or benign). To determine two sets of mass contours, two approaches were applied. A confined geographical area method and a dynamic programming-based method are used. Additionally, simplified contours (modeled as ellipses) were used to extract a set of 6 characteristics for identification of mass margins. The following are the sets:

1. Assessment of spiculation (depending on texture features).
2. Spiculation determination (terms of relative gradient orientation).
3. Two measurements s of mass margins' fuzziness.
1. The variation coefficient of edge strength.
2. Background region.
3. The contrast between foreground region.

Then, three popular classifiers were implemented to predict a dataset of 300 tumor diagnoses depend on the textures extractions . The classifiers are the support vector machine, Fisher's linear discriminant, and Bayesian classifier. Lastly, comparisons were conducted among the systems to evaluate each system's performance in diagnosing breast masses.

The authors in [60] developed a machine learning depend on CAD able of determining, classifying, and segmenting the tumor in mammograms images. Furthermore, preprocessing strategies is suggested to take away muscle region, artifacts, and noise. It is worth mentioning, keeping muscle regions can lead to a high false-positive rate. Then, the stage image processing is transfer to 512×512 image to improve the system's efficiency and counter the large resource requirement.

The experts in [61] presented an adaptive statistical data analysis approach (DAA images). The flat cap transform is used for nucleus localization and screen resolution improvement. Discrete wavelet transform and multiscale zone, then used in conjunction to identify ROIs and pinpoint their precise area. Another double dividing models is then utilized to split occupied cells for increasing prevalence and accuracy. Curve identification in Contour Grid Points (CSS) and dynamic theoretical morphogenesis are included in the DSSM.

Finally, containing more than 3600 cells, the proposal has been tested on 68 BCH images.

In [62] [62] proposes that pixel-wise area identification be done using a fast patrolling deep convolutional neural network (fCNN). The fCNN eliminates the conventional CNN's unnecessary operations without loss of performance. In our tests, segmenting a scene with a size of 1000 by 1000 pixels took only 2.3 secs.

To derive ROI, trainable segmentation and an improved threshold-based model were proposed in [63]. A hybrid segmentation approach was established for the pectoral muscle and boundary region breast. The establishment was based on Machine Learning (ML) and thresholding techniques. Then, the breast region was highlighted for breast boundary estimation, and it was performed by taking off wavelet transform bands. Determining initial breast boundary was achieved using a new thresholding technique. Small objects were deleted to correct the overestimated boundary. This procedure was performed by employing Morphological operations and masking. For the segmentation process, there is significant progress in the medical imaging field. The progress focused on developing efficient and accurate ML methods. The literature highlights the ML methods' role in achieving efficient and further accurate segmentation methods. In the research, an ML technique was built to determine ROI and pectoral muscle region. The technique was based on the feature of Histogram of Oriented Gradient (HOG) with classifiers of neural network. The test of segmentation approach has been conducted by using100, 200 and 100 mammogram images.

Finally, the authors of [64] developed an automated mammogram images detection approach based on optimum region growth. Furthermore, the initial amount locations and thresholds are optimally generated using a swarm optimization approach (Dragon Fly Optimization (DFO)). Texture features are recovered from segmented pictures using GLCM and GLRLM algorithms. The attributes are then supplied into a (FFNN) classifier (educated using a back propagation approach). It's worth noting that the FFNN can distinguish between benign and malignant images. Finally, photographs from the DDSM database were used to assess the performance of the suggested detection approach.

3. METHODOLOGY

The developed CAD system in this chapter is devoted to the development of a method for object segmentation and a classification algorithm (for example, tumors) of MRI images based on the use of the developed computational procedures. Algorithms of threshold iterative segmentation of objects in MRI images are investigated. It is known that it is very difficult to select a suitable global threshold for obtaining an ideal initial contour due to differences in gray levels in the area of pathology in images (for example, breast tumors), as well as for an uninfected area, given the high correlation between adjacent areas of successive images (MRI and CT). Detecting and classifying the edges of objects of interest (brain or breast tumors) on MRI medical images help clinicians during diagnosis. With segmentation, it is possible with a high degree of accuracy to define the area (outline) of these areas (tumors and normal areas of the breast). It has been shown that the results obtained are accurate and adequate, since there are many methods, but the methods that provide the best results have been selected.

3.1. PROPOSED METHODOLOGY

The quality of images produced using medical devices determines the processing outcome. The noise created by the technological elements of the gadgets has been proven in most examples by the testing results of several datasets.

There are many methods used in the detection or segmentation of breast tumors in different systems. Our proposed algorithmic procedure works on objects' segmentation (i.e., tumors of breast cancer) with high accuracy and their classification. Since the results of the analysis of medical images can be distorted since the photographs include a lot of noise, to improve the diagnostic accuracy on MRI images, we suggest using the following algorithm for processing local objects (tumors) on MRI images, as shown in Figure 3.1.

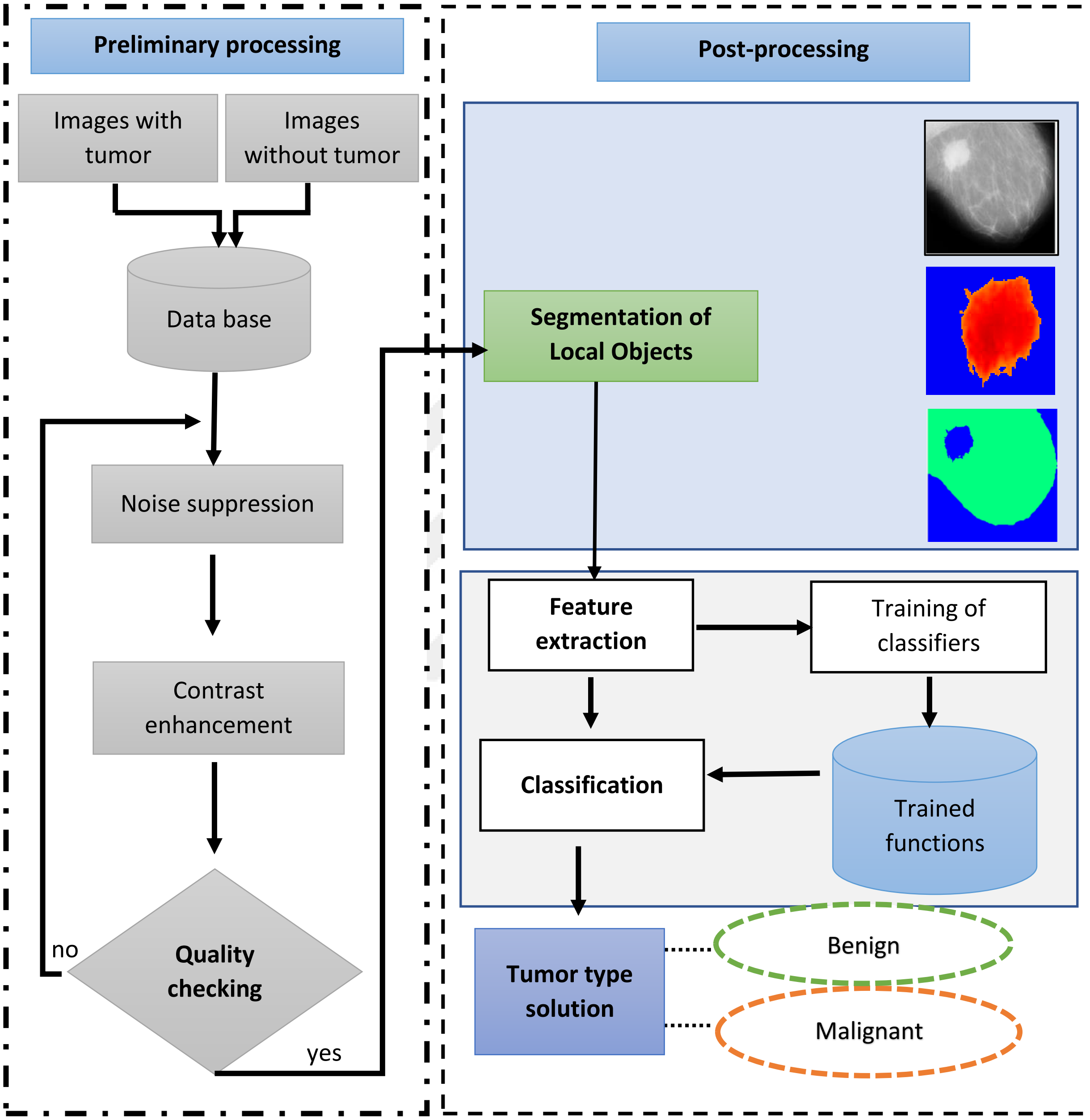

Figure 3.1: Block diagram of the classification of local objects (tumors) for the analysis of medical images of MRI (breast)

Usually, doctors refer the patients to the image and draw up an image analysis report to determine the type of tumor. Our proposed method will help the doctor diagnose cancer patients, and enable them also to train the system based on few data. Then they utilize the system to obtain a report on the patient's condition after testing the data.

The image section that contains the tumor is usually further intense than the remaining parts of the image. In this case, the main steps of the tumor detection algorithm are used, which are implemented in the developed algorithm and program code. Meantime, further processing can be performed for the part with the anticipated content of the object of interest. The processing considers the metrics necessary for the analysis.

3.1.1. Improving The Contrast of Images

The main function of sharpening phase is to improve the images contrast of the local studied area (tumors of breast cancers) on MRI. Additionally, a shape is created suitable for more processing by machine vision systems or humans. Additionally, specific MRI parameters are improved by preprocessing, such as the following [77]:

1. Signal to noise ratio.
2. Improve medical images appearance.
3. Delete insignificant noise and unwanted areas in the background.
4. Smooth area's inner part.
5. Preserve its edges.

Then, we apply adaptive contrast enhancement based on the modified equation(described in [65]) to get a better accuracy and less of false segmentation. Consequently, improving the purity of the original MRI scans. However, the main obstacle is poor image quality to extract, analyze, recognize efficiently, and quantitively measure parameters. Due to some imperfect imaging process characteristics, medical images are usually made impured by impulsive, multiplicative, or additive noise. The authors in [37] proposed using Contrast Balance Enhancement Technique (CBET) technology to get better contrast of highlighting the interest area. It is worth mentioning, the area of interest requires contrast during medical imaging.

The articles [66, 67] described the Contrast Limited Adaptive Histogram Equalization (CLAHE) technique. The technique aimed to improve the characteristics and determine better medical image characteristics, leading to adequate diagnosis. For image enhancement, the is another interesting approach which is Unsharp masking. The goal is to improve edges and detail; however, using a high-frequency emitter makes this technique very sensitive to noise. In his work [68], the author showed that invariant contour transform (STICT) improves the MRI scans quality.

In the suggested method, we use the algorithm (BCET). Image contrast can be compressed or stretched without altering the shape of the source image's distribution (I_{old}). In the quick fix, a parabolic function is obtained from the input image. The parabolic function equation is written as follows:

$$I_{New} = a \cdot (I_{old} - M)^2 + N \ . \tag{3.1}$$

The coefficients a is derived from the input. Whereas m and n are determined from the minimum output image value (I_{New}), the maximum source image value. The following equation calculates the value of the average final image:

$$m = \frac{h^2 \cdot (P-Q) - s \cdot (P-Q) + l^2 \cdot (P-Q)}{2 \cdot [h \cdot (P-Q) - e \cdot (P-Q) + l \cdot (P-Q)]}, \tag{3.2}$$

$$a = \frac{P-Q}{(h-l)(h+l-2b)}, \tag{3.3}$$

$$N = Q - a(l-b)^2, \tag{3.4}$$

$$s = \frac{1}{N} \sum_{i=1}^{N} I_{Old}^{2}(i) \ . \tag{3.5}$$

where h and l are the input image's highest and lowest values, respectively. P and Q are the output image's highest and lowest values, respectively. The average of the source images is denoted by s, whereas the mean square sum of the image pixels is denoted by e.

3.1.2. Object Segmentation Method

Commonly, Subdivision of images is implemented to locate boundaries and objects (curves and lines, etc.) in images. Segmentation of medical images to detect a local object (breast tumors) using magnetic resonance imaging (MRI) scans is a crucial act for making the correct treatment decision in a short time [69, 70].

Image segmentation is the most important part of medical imaging and the procedure for isolating an area of interest (ROI) using a semi-automatic or automatic process. In the literature, several image segmentation techniques were implemented for medical purposes to segment tissues and organs of the body. Some applications include edge detection on coronary angiograms, surgical planning, surgery simulation, detecting and segmenting of tumor, breast and animal development studies, functional mapping, automatic blood cell classification, mammogram mass detection, image registration, cardiac segmenting and analysis, images of the heart, etc. [71, 72, 77].

The dissertation developed a threshold iteration method for segmenting objects (tumors) and non-infected areas (breast) in MRI and CT images based on improved Otsu and C-means fuzzy clustering, as shown in Figure 3.2.

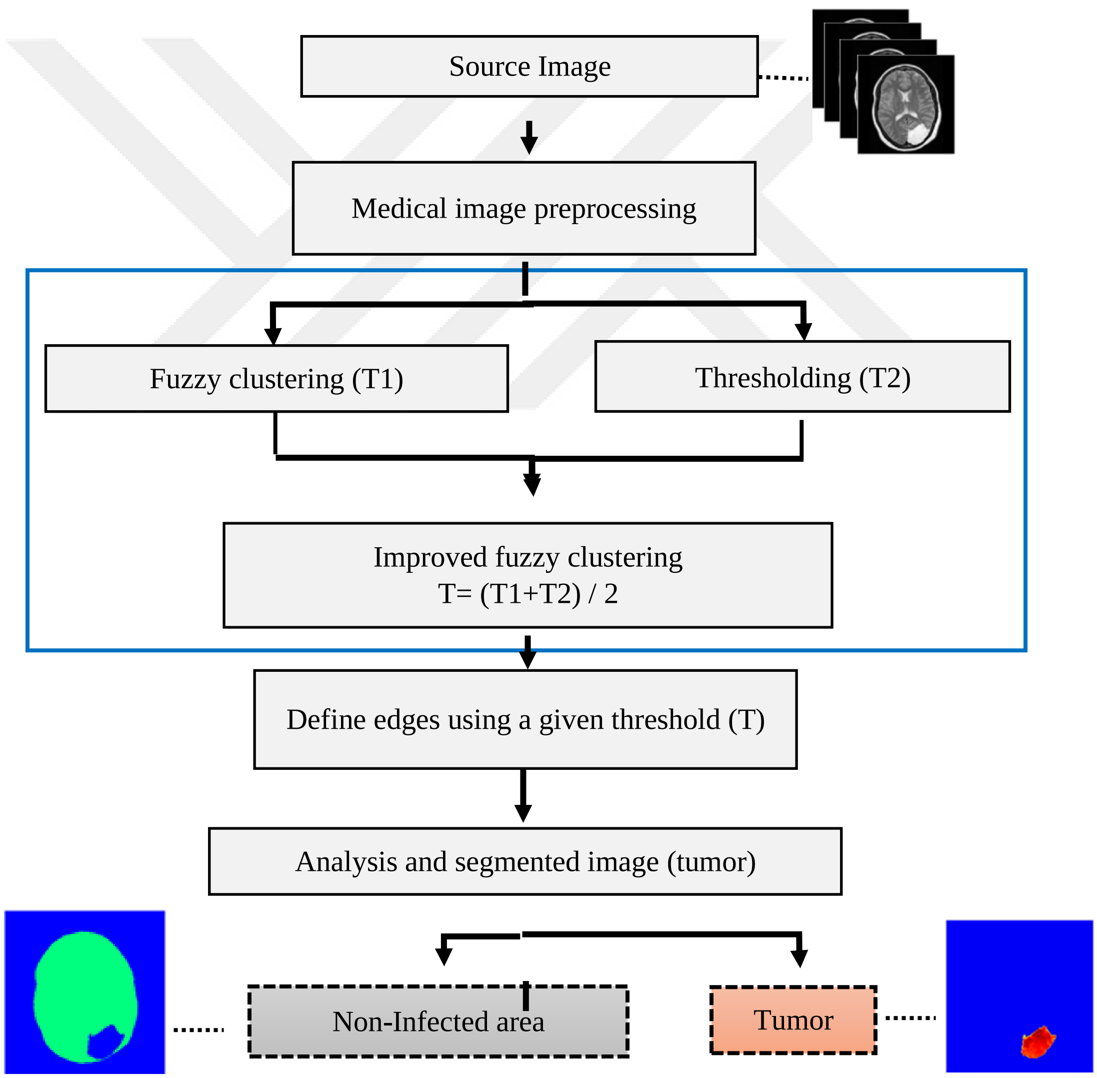

Figure 3.2：Block diagram of the developed method of threshold fuzzy C-averages

Let L black and white level [1,2, ..., L] express the intensity of the gray level image. xi denotes the number of points with a gray level *p (i)*. $X = x_1 + x_2 + \cdots + x_L$ refers to the total number of points. The gray level image's histogram is considered as a probability distribution of occurrence:

$$p(i) = \frac{x_i}{X}, x_i \geq 0, \sum_{i=1}^{L} x_i = 1. \tag{3.6}$$

Image pixels are comprised of two parts C_0 *and* C_1 Foreground and background with a threshold value of t. While C_0 re-represents pixels within levels [1,2, ..., t], C_1 presents pixels within the levels [t + 1,… L]. The following equations define the class and middle occurrence probabilities, respectively.

$$w_0 = w(t) = \sum_{i=1}^{t} p(i), \tag{3.7}$$

$$w_1 = 1 - w(t) = \sum_{i=t+1}^{L} p(i), \tag{3.8}$$

$$\mu_0 = \sum_{i=1}^{t} \frac{i.p(i)}{w_0} = \frac{1}{w(t)} , \tag{3.9}$$

$$\mu_1 = \sum_{i=t+1}^{L} \frac{i.p(i)}{w_1} = \frac{1}{1-w(t)} \sum_{i=t+1}^{L} i.p(i) . \tag{3.10}$$

The overall average is defined:

$$\mu_T = \sum_{i=1}^{L} i.p(i). \tag{3.11}$$

and then we can find:

$$\mu_T = w_0\mu_0 + w_1\mu_1 , \tag{3.12}$$

where w_0 and w_1 - denote the probabilities of the front and background areas. In addition, μ_0, and μ_1 represent the average gray level value of the foreground and background gray image, respectively. Where the entire gray level image is defined as μ_T,.

The variant between the classes σ_B^2 of the two parts C_0 and C_1 can be rewritten as:

$$\sigma_B^2 = w_{0\,(}\mu_0 - \mu_T)^2 + w_{1\,(}\mu_1 - \mu_T),^2 \tag{3.13}$$

and the quality threshold t* is selected to maximize σ_B^2 :

$$t^* = \arg\max \sigma_B^2 , \; 1 \leq t \leq L. \tag{3.14}$$

When the distribution for class C_K *(k = 0 or 1)* is between regions with different characteristics, the median is known to be a reliable estimate compared with mean gray scale. To find the median value of the replacement of the mean can be obtained as t*, which is quite reasonable given the presence of the C_K distribution in comparison with these thresholds chosen by the Otsu algorithm.

Therefore, the total median level m_T can be replaced instead of the overall mean μ_T. Similar to the mean μ_T of the entire image. The middle values μ_0 and μ_1 can also be replaced with the middle gray levels m_0 and m_1 of the front part C_0 and the rear part C_1, respectively. The variant between classes σ_B^2 of two parts C_0 and C_1 can be rewritten as:

$$\sigma_B^2 = w_0 (m_0 - m_T)^2 + w_1 (m_1 - m_T)^2, \tag{3.15}$$

and the quality threshold t* is selected to maximize σ_B^2 :

$$t^* = \arg\max \sigma_B^2 , \ 1 \leq t \leq L. \tag{3.16}$$

2.4. OBJECT DETECTION AND CONTOURING

Various algorithms can generate contour map, as example Sobel, Prewitt, Roberts, and more complex ones, as Canny, shearlet, wavelet, and LoG. The Enhanced Canny Operator's Advanced Low-Frequency Edge Detection method is the most efficient detector of many edge detection operators in the image processing domain (described in 1.5.1 above).

This method is capable of perceiving a wide range of image edges because it exactly meets the general contour detection criteria, and the deployment process is fairly straightforward [72]. The improved Canny operator is used after dividing the image into a succession of assumption is called class conditional (implementing the developed segmentation method). It is depended on the pixel gradient value and defines the shallow edge. However, the image contains homogeneous areas. Here, we describe the step of the method in detail. Firstly, the original images are smoothed using a Gaussian filter. Additionally, the direction and magnitude of the gradient are obtained for image pixels. Secondly, the border pixels (extreme pixels) are selected. If the gradient value of the pixel is larger than its two neighbor in the opposite direction of the gradient, the pixel is deemed a boundary pixel.

3.1.3. Feature Extraction

The quality of the extracted features is crucial in the accuracy of object classification. We have proposed a classification algorithm for distinguishing features of a segmented object using gray level interaction matrix (GLCM) and discrete wavelet transform (DWT). This step is essential in the computational technique since the classification process accuracy relies on the extracted features' quality. Input images (MRI) are taken in the computational procedure and gives a discrete wavelet transform (DWT) for MRI. The DWT coefficients are then analyzed by calculating 13 statistical values that represent the extracted features.

In calculating the DWT matrix, various offset values are used in this research. Nevertheless, for the offset values, the best classification accuracy was obtained [2 0] and [2 0, 0 2]. Accordingly, we call these values as "offset one" and "offset two", respectively. The step of extracting a contour element is the same for both the training phase and the testing phase.

The Gray Level Cooperation Matrix (GLCM) is a reliable way to analyze images statistically. According to second-order statistics, it is used to evaluate the characteristics of images. The GLCM matrix is denoted as the two-dimensional joint probability matrix between the pairs of pixels above the image (I) as the distribution of the joint values at a given offset (dx, dy) for an N × M image:

$$C_{dx,dy}(i,j) = \sum_{p=1}^{N}\sum_{q=1}^{M}\begin{cases}1, & if\ \ I(p,q) = i\ and\ I(p+dx, q+dy) = j\\ 0, & otherwise\end{cases} \quad (3.17)$$

Selected characteristics are as follows [73, 74]:

1. F1: Energy.
2. F2: Contrast.
3. F3: Correlation.
4. F4: Autocorrelation.
5. F5: Entropy.
6. F6: Homogeneity.
7. F7: Mismatch.
8. F8: Cluster Shade.
9. F9: Prominence Cluster.
10. F10: Maximum Probability.
11. F11: Sum of Square.
12. F12: Moment of Inverse Difference.
13. F13: Cumulative Mean.
14. F14: Cumulative Deviation.
15. F15: Cumulative Entropy.
16. F16: Variable Deviation.

17. F17: Variable Entropy.
18. F18: Informational Correlation Dimension.

For better classification results, GLCMs are generated for various offsets (2 to 4 pixels) and angles (0 °, 45 °, 90 ° and 135 °).

The isolated features (based on the region of the object - tumor) and selected from the segmented images are then classified using neural network techniques to diagnose whether the patient has a (benign tumor) or (malignant tumor). Implementing a combination of methods improves the accuracy of results and estimates.

3.1.4. Classification of Local Objects (tumors)

Consider the binary classification process, and the detected tumor can be determined as stage malignant or benign by using the classifier. To fulfill its role, the extracted elements and the previously acquired knowledge are used by the classifier. A probabilistic neural network (PNN) is used as an extracted feature-based object classifier (breast tumors) using the GLCM transform and a support vector algorithm (SVM) - as an extracted feature-based breast tumor classifier using DWT.

3.1.4.1. Classification Using PNN

The probabilistic neural network model was used in this study (PNN). This approach is simple to put into practice. Furthermore, it has been frequently applied to categorization issues. When displaying the input, the distance from the input vector to the training vectors is calculated in the first layer. Next, the layer creates a vector with elements that show how the input vector is close to the training input.

To obtain a vector of possibilities as net output, the contributions of each class are summarized in the second level. At the output of the second level, the transfer function has competed by selecting the maximum of these probabilities. Accordingly, the transfer function is 1 for this class and 0 for other classes [6, 16].

The Parzen Probabilistic Neural Network (PPNN) is considered a simple kind of neural network. The PPNN is deployed for classifying data vectors. Based on Bayesian theory, the classifiers are fast, easy to learn. The data (obtained by the parcened window approach) is used to estimate the posterior probability density [75]. A certain class of data distribution can obtain good classification results. The bayesian equation is used by Bayesian classifiers to anticipate the probability density P (w_i |x):

$$P\left(w_i \frac{1}{x}\right) = \frac{P_{(x\ /w_i)}\ P(w_i)}{\sum_i P_{(x\ /w_i)}\ P(w_i)}\ . \tag{3.18}$$

It is obvious that the probabilities P (wi) and P (wi |x) must be defined in this method. These pdfs are parameterized using the technique, whereas the other is to evaluate them from the data. For a given window size, the probability of defining a window is estimated by the frozen window technique. Additionally, the technique estimates the function on that window, which is a hypersphere with a truncated Gaussian function inside. It is obvious that the window function should have an integral (hypervolume under the function) equals to one to keep the scale in the evaluative pdf.

Hence, the PPNN algorithm can easily compose a probability density function (PDF) estimate with a Bayesian classification and Parzen window. Specific derivatives are not given in this brief explanation (available in [24]).

Accordingly, the architecture of Parzen PNN comprises of four-layer Neural Network. The connection among the layers are as follows: As shown in Figure 3.3, the first and second layers are loosely connected. There are c neurons on the output layer, which denotes the number of classifier classes.

The following is the first level weights train: Normalizing each sample and making its length unitary. Additionally, each sample value becomes a neuron with normalized values in the form of weights w.

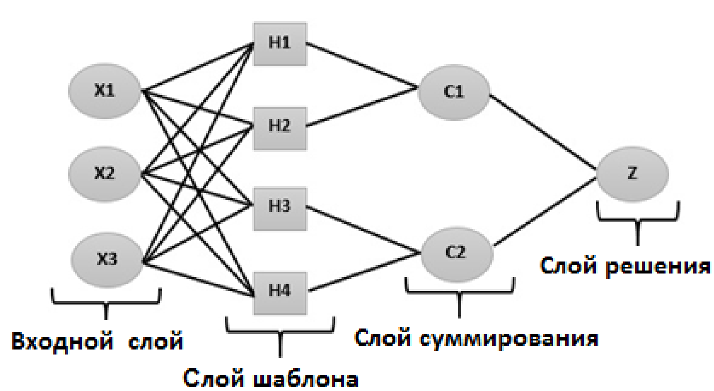

Figure 3.3 : A four-layer PNN architecture for n training cases from two classes.

Accordingly, the input data x is multi-point. The following equation defines the weights that receive the network (network) activation signal:

$$net = w^{x^T} \tag{3.19}$$

The exponential nonlinearity is then calculated to generate synaptic activation (act) signals according to the equation:

$$act = \exp\ [sigm\ \left(\frac{net+1}{2}\right)] \tag{3.20}$$

In the process of training, each neuron of the first layer is connected to a neuron of the output layer (which belongs to its class) with a weight of 1. Whereas in the process of classification, the activation signals from all neurons of the first layer are sum up at the output neuron of each class. This means that the largest output value chooses the input data class

3.1.4.2. Classifying Local Object Using SVM

The goal of this phase is to develop a CAD system for identifying breast malignancies on a breast CT scan. The approach proposed can distinguish between two types of breast tumors (benign and malignant). The system's three main phases are segmentation, extraction of features and identification, and classification. We employed the known segmentation approach for picture segmentation and the discrete wavelet transform for feature extraction (DWT).

As seen in the equation, the SVM algorithm creates a hyper - plane that is split into 2 classrooms:

$$f(y) = Z^T\ \emptyset\ (y) + b, \tag{3.21}$$

where Z and are hyper - plane variables, and f (y) is the function that maps y to a safety and high. The Gaussian component of the kernel of the nonlinear SVM [46, 47] is given by equation (3.22). It is used for calculating both classification and generalization optimal solutions. Additionally, the form (2.23) defines its extended classification function:

$$k\ (y_i\ , y_j) = \exp\left[-y\ ||y_i - y_j||^2\ \right], \tag{3.22}$$

$$k\ (y_i\ , y_j) = \sum_{i=1}^{N} \sum_{X_i\ \in M_j} \left(exp\left[-y\ ||y_i - y_j||^2\ \right]\right)\ , \tag{3.23}$$

where *yi* and *yj* are the objects *i* and *j*, and y is the curve variable that controls the smoothness of the border region.The choice of functions with the ability to change the class of the nucleus makes the SVM algorithm the default choice for classifying breast tumors (benign or malignant).

4. COMPUTATIONAL EXPERIMENTS AND DISCUSSIONS

In this pilot study, we used two datasets to analyze objects (breast tumors). The first dataset is the Digital Imaging Dataset (DICOM) [55]. The researchers reviewed 150 images with breast tumors taken from the DICOM dataset for analysis purposes.

Furthermore, the Breast-Web dataset [76] is the second used dataset consisting of complete 3D breast MRI data modeled in three sequences of modalities, namely T1-weighted MRI and T2-weighted MRI. In this dataset, 15 of the 48 included images contain breast tumors. An additional set of breast tumor data collected from radiological specialists included image samples of 10 patients with 6 images for each patient. For breast MRI in the pilot study, 75 images were selected from MRI scans and a digital database for screening mammography (DDSM) [59, 78].

As shown in Figures 4.1, the results of using different implementations of BCET, instead of using different thresholds, since the MRI scan contains different contrast and in this case segmentation rather than an exact tomogram.

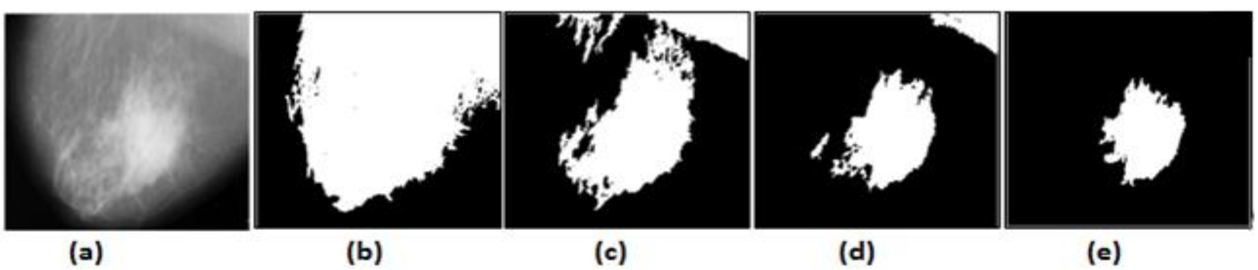

Figure 4.1: An example of segmentation of an object (breast tumor) for varieos mean values of balance contrast : a) original image, b) BC=110,
c) BC =95 , d) BC = 75, e) BC = 65

Figure 4.2 illustrates an example of contour map processing and creation using the suggested approach. The figure for a breast tumor includes the following images: (a) the actual image; b) and

c) preprocessing images; d) the result of our technique's segmentation (FCMT); e) the result after the Otsu threshold; f) the result of the method created; g) a combination image with a colour chart; h) the end-edge map for the breast and tumor areas.

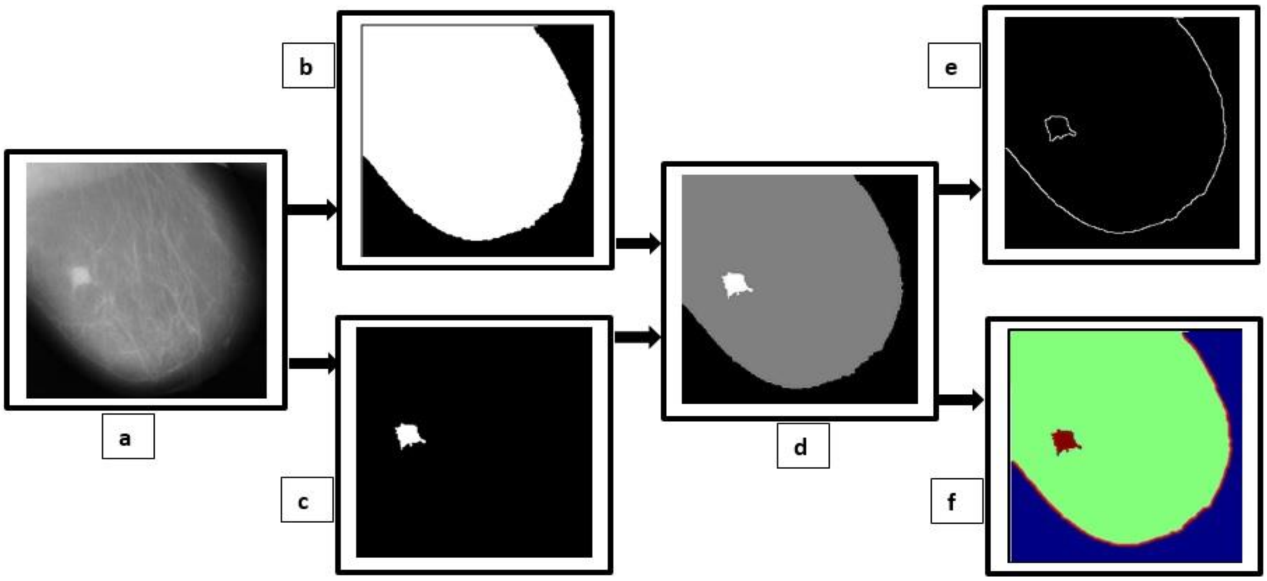

Figure 4.2: An example of combined segmentation and contour detection of an object (breast tumor)

The experiments were performed on a variety of 256 x 256 images. Here are the results of some of the segmentation and detection of breast tumors. Examples of breast MRIs obtained in the course of a computational experiment on segmentation and detection of breast tumors are shown in Figure 4.3. It can also be seen that the brightness and contrast of the image varies from image to image, where the top row shows the original images (Digital Database for Screening Mammography (DDSM)), sorted from left to right.

The first column represents the original images, the second column represents the image results after the preprocessing step and is shown in color using a color map as explained in the section above. In this version of the calculation of the image segmentation by areas - in the third column, and in the last column - the result after segmentation and processing (final contour). By differentiating between non infected cells and tumor cells, it also helps in calculating the area of the tumor, the area is calculated in pixel units.

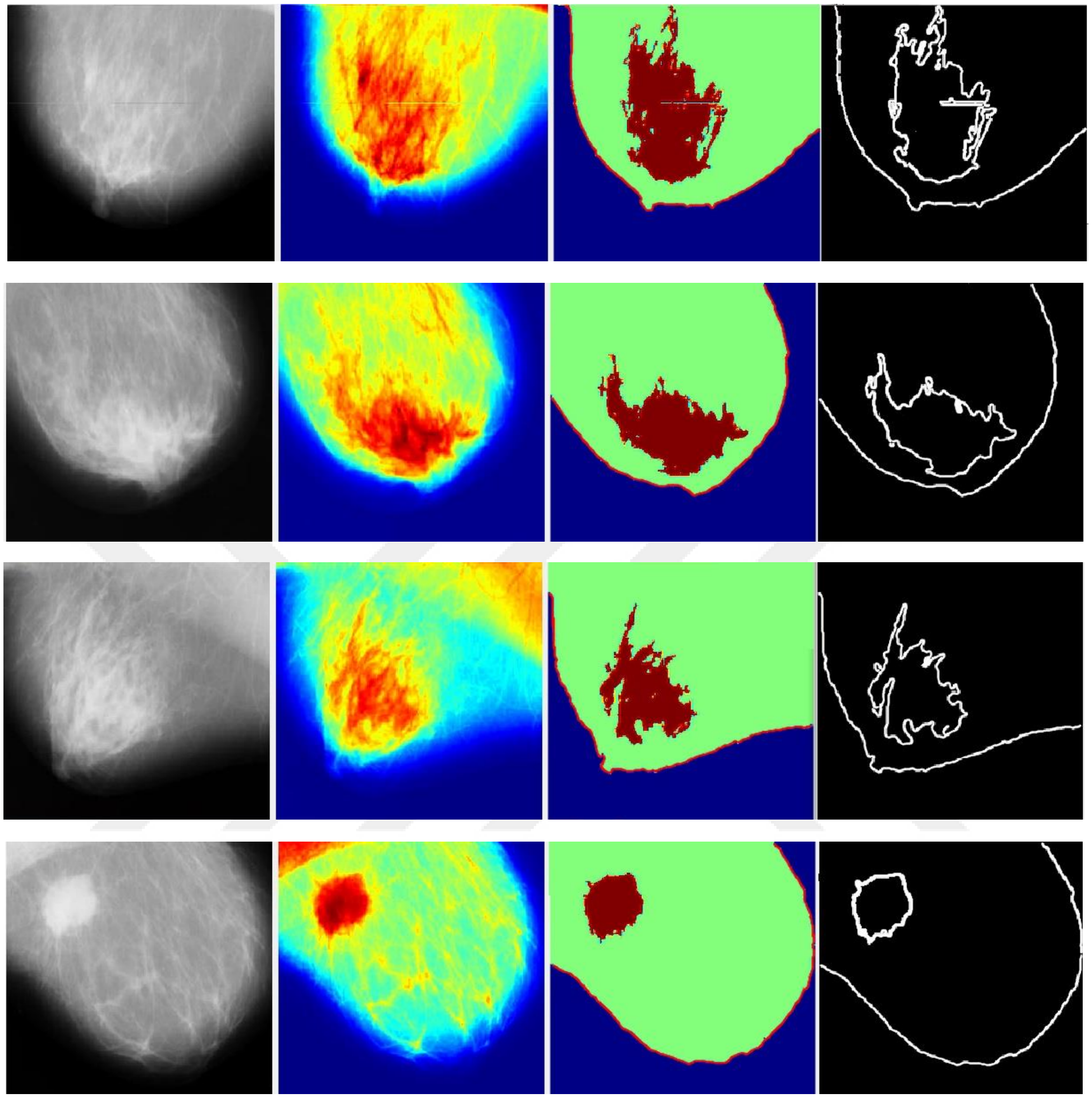

Figure 4.3: Some results of applying the method to determine the position of the object (breast tumor)

Where the methods in [1, 21, 147, 152, 155] and [39, 43, 94] include some non-neoplastic area on the Friday segmented image, ambiguous for diagnosis (no tumor boundaries and normal areas of the breast). Our method detects the tumor area (as well as the normal breast in the original input image) successfully with a color result as shown in Figures 4.3. Visual analysis makes it clear that our algorithm is able to segment tumors and normal areas better than other methods.

The following parameters were used to assess the tumor’s correctness and reliability and the map of the normal area of the breast and the edge of the mammary gland was obtained by our method:

1. Structured similarity index (SSIM).
2. Mean square error (MSE).
3. Peak signal-to-noise ratio (PSNR) in dB.
4. Pixel Detected Percentage (PCD).
5. Pixel Not Detected Percentage (PND).
6. False Positive Rate (PFA), Merit Score (MS).
7. Sensitivity and Accuracy.

These seven metrics mainly depend on TP, TN, FP, FN values:

- True positive (TP): Refers to pixels number that correctly identified as the tumor border;
- Negative (TN): Denotes pixels number that correctly detected as the background;
- False positive (FP): By its name, it is the number of pixels falsely identified as the border of the tumor;
- False negative (FN): Considers as the number of pixels falsely detected as the background;

The Structural Similarity Index (SSIM) is a perceptual metric where data transmission or compression loss or any other image processing technique causes degradation in image quality. The following equation defines SSIM:

$$SSIM(x,y)=\frac{(2\mu_x\mu_y+C_1)(2\sigma_{xy}+C_2)}{(\mu_x^2+\mu_y^2+C_1)(\sigma_x^2+\sigma_y^2+C_2)}. \tag{4.1}$$

A higher SSIM value refers better retention of brightness, structural content, and contrast.

The accuracy of an image or signal is usually measured with Root mean square error (MSE). The purpose of measuring the accuracy of an image or signal is to determine the similarity between two images, and it can be measured by providing a quantitative estimate. In calculating the MSE, one of the images is assumed to be the original, whereas the other is distorted or processed in one way or another and is defined as:

$$MSE = \frac{1}{N}\sum_{i=1}^{N} E_i^2 = \frac{\|E\|^2}{N} \quad . \tag{4.2}$$

Peak Signal-to-Noise Ratio (PSNR) is used to evaluate image reconstruction quality. It is calculated as follows:

$$PSNR = 10\log_{10}\left(\frac{(2^n - 1)^2}{MSE}\right) = 20\log_{10}\left(2^n - 1\right) - 20\log_{10}\left(\frac{\|E\|}{\sqrt{N}}\right). \tag{4.3}$$

Higher PSNR and Smaller MSE refer to better signal to noise ratio.

The Figure of Merit (MS) is also used to evaluate edge detector performance. It utilizes the distance between all pairs of points, quantifying, with precision, the difference between the contours. The similarity between the two contours is measured with the MS score that can be written as follows:

$$FOM = \frac{1}{\max(RE_{Cnt}, AE_{Cnt})} \cdot \sum_{i=1}^{AE_{Cnt}} \frac{1}{1 + \alpha \cdot d_i^{\,2}} \,, \tag{4.4}$$

where RE_{Cnt} и AE_{Cnt} – number of ideals (standard) and real point on the edge;

di is the distance between the pixel at the edge and the nearest pixel at the edge of the reference; α - empirical calibration constant (used α = 1/9, optimal value).

The measuring range is from 0 to 1, and the optimal is the maximum value. The following equation represents the Sensitivity and is defined as follows:

$$Sensitivity = \frac{TP}{TP+FN}. \tag{4.5}$$

The fraction of the true results represents the accuracy. Whereas the percentage of how many objects and background pixels were accurately detected is denoted as Precision. The measurement ranges from 0 to 1. The output signal becomes equal to the input signal when the accuracy value is 1. Thus, the accuracy is written as follows:

$$\text{Accuracy} = \frac{TP+TN}{TP+TN+FP+FN}. \tag{4.6}$$

It is clear from the observed results that detecting the normal area and tumor of the breast and the MRI of the breast is accurate and fast compared to manual detection performed by clinical specialists.

The most commonly used metrics in the medical image segmentation and classification technique using neural networks are the Intersection Over Union (IoU) Metric metric described in Equation (4.7) and Dice Similarity Coeffcient (DSC) (Equation (4.8)). The IoU or Jaccard index consists of quantifying the percentage of overlap between the truth mask and the predicted output mask. This metric is closely related to the dice similarity coefficient, which is often used as a function of accuracy during training:

$$IoU = \frac{TP}{TP + FP + FN} \quad . \tag{4.7}$$

$$DSC = \frac{2TP}{2TP + FP + FN} \quad . \tag{4.8}$$

The assessed performance factors also show that it improves the PSNR, MSE, and SSIM parameters. The suggested technique gives accurate and rapid object detection (breast tumors) and determines the exact location of the normal areas and tumors in the MRI images. Tables 4.1 outlines the analysis of obtained images' efficiency at the edges by calculating the tumor area and the area without pathology (breast).

Table 4.1: Parameters for analyzing the effectiveness of the identified tissues and the area of removed tumors and areas without pathology.

Images	**Highlighted tumor area (pixel)**	**Highlighted area of normal breast (pixel)**	**Tumor size %**	**PSNR**	**MSE**	**SSIM**	**DSC**	**Execution time in seconds**
Image 1	8940	41272	22%	68.990	1.920	0.9565	0.9562	24.1257
Image 2	7025	39541	18%	64.004	1.35	0.9675	0.9639	23.5863
Image 3	2029	43394	5%	65.066	1.215	0.9700	0.9698	25.5863
Image 4	4311	45380	9%	64.03	2.172	0.9663	0.9750	23.02236
Image 5	1956	46811	4%	66.256	1.245	0.9726	0.9658	26.8860
Image 6	15561	44600	35%	67.504	1.757	0.9623	0.9785	24.0563

The following studies were conducted to demonstrate that the suggested technique is robust and has more accuracy of detecting edges capability to moderate noise levels. The first research compares the proposed method with classical approaches of edge detectors such as, Canny, Sobel and complex LoG, Prewitt and Roberts methods.

During the research, the assessment scores are calculated using reference images created by a medical examiner. A comparison of several methods of forming a contour representation (edge map) of breast tumors for the first image models shown in Figures 4.3, as well as those given in Tables 4.2, is demonstrated.

Table 4.2: The evaluation of edge maps generated by tumor and normal breast cells by various approaches and developed method

Image Model	Methods	MS	Sensitivity	Accuracy
Image A	The developed method	0,9158	0,9518	0,9744
	Classic Canny	0,5632	0,2547	0,8452
	Prewitt	0,4643	0,0928	0,7489
	Roberts	0,4362	0,0564	0,7376
	Sobel	0,5282	0,0647	0,6379
	LoG	0,5664	0,05742	0,6031

The suggested technique improves the accuracy of obtaining a map of the edges of the item of interest (tumor region and normal areas) by 3-7 percent on average. Furthermore, the proposed technique indicates a reduced fraction of pixels that are incorrectly identified as breast tumor edges. For noise levels less than 10%, the difference is less than 1%. The sensitivity index, on the other hand, shows a more significant drop while remaining within acceptable limits.

Table 4.3 shows an overview of contemporary approaches (since 2016) for different medical distribution - based issues that use a deep neural network and other delineation algorithms.

Table 4.3: Modern methods using various algorithms in the segmentation of medical images.

Year	Methods	Segmentation application	Modality	Accuracy (%)	Metric
2018 [14]	Genetic Algorithm	Brain tumor	MR images	92.03	DSC
2017 [38]	2 conductive U-Nets	Breast tumor	MRI-T1	94.30	DSC
2019 [43]	U-Net	Breast tumor	MRI-T1	76.14	IoU
2019 [70]	Fuzzy C-mean	Brain tumor	CT images	91.18	DSC
2016 [100]	V-Net (Volumetric U-Net)	Breast tumor	MRI (T1, T2)	82.39	DSC
2019 [147]	CNN Approach	Breast tumor	MR images	91.05	DSC
2017 [148]	CNN Approach	Brain tumor	MR images	90.50	DSC
2018 [161]	Bayesian CNN	Primate Brain Extraction	MRI-T1	95.00	DCS
The developed method	FcMT	Breast tumor	MR and CT images	96.85	DSC
				94.74	IoU

The developed approach is very accurate, as shown in Table 4.3, with just a 2-3 percent error in the delineation of medical scans.

To test the accuracy of the SVM and PNN classifiers, they were trained on a combined collection of MRI images (from the digital imaging in medicine (DICOM) dataset).

Tables 4.4 and 4.5 present the results and descriptions for the categorization of breast tumor

Table 4.4: SVM classifier of accuracy of breast tumor on CT images.

Images	No feature highlighting			With feature extraction		
	Quantity images	Classification %		Quantity images	Classification %	
		correct	Not correct		correct	Not correct
Tumor images (benign)	42	92.58	7.32	42	99.85	0.15
Tumor images (malignant)	36	95.65	6.35	36	98.96	1.04
Total amount	78	95.11	13.67	78	99.02	1.17

The average classification accuracy of the experimental studies has resulted in 99% with feature extraction and 95% without feature extraction, as can be noted

The errors in the classification of benign and malignant tumors in breast MRI and CT images are about 1-2% with feature extraction and 3-4% without feature extraction.

Table 4.5: of PNN classifier of breast tumor on CT images.

Images	No feature highlighting			With feature extraction		
	Quantity images	Classification %		Quantity images	Quantity Images	
		correct	Not correct		correct	Not correct
Tumor images (benign)	20	94.88	3.12	20	98.96	1.04
Tumor images (malignant)	20	93.91	4.09	20	98.97	1.03
Total amount	40	94.79	7.21	40	98.96	2.07

The average classification accuracy of the experimental studies has resulted in 98% with feature extraction and 95% without feature extraction, as can be noted from The errors in the classification of benign and malignant breast tumors on MRI images are about 1-2% with an extracted feature and 3-5% without feature extraction.

5. CONCLUSIONS AND FUTURE WORK

5.1. CONCLUSIONS

Breast tumor (cancer) in women is considered the most often cancer diagnosed. Despite the fact that women with cancer have the second highest death rate, early diagnosis substantially increases the chances of survival. As a result, it is critical to create new improved mammography technologies.

The BCET method is proposed to enhance contrast and highlight the area of interest in medical images. The Otsu threshold procedure is achieved by replacing the total mean _T with the total median level m T of all points in the entire gray level image, similar to the mean _T of the entire image, the average values _0 and _1 can also be replaced by the middle gray levels m 0 and m 1 of the front part C 0 and the back part C 1, respectively. A new method of segmentation by groups of objects has been developed, which is characterized by the creation of a new threshold for segmentation of objects using a combination of the threshold value of the improved Otsu algorithm and fuzzy clustering, which significantly increases the speed and improves the accuracy of segmentation and classification of objects by 2-3% compared to modern methods medical segmentation (2016-2019).

In the developed segmentation method for individual objects, a scalar parameter for the selection of objects is described - the threshold distance between the histograms of the intensity distribution. An approach is proposed for dividing into separate objects by combining super-pixels.

The novel approach presented, its implementation in Matlab, and its assessment on a dataset of 209 breast mammography images were all detailed in the dissertation. The emphasis was on seeing how the approach performed under various situations rather than producing an overall accuracy result. The overall objective of this thesis was to enhance breast cancer screening by assisting radiologists in the categorization of breast lesions using neural networks and logistic regression.

Another goal of the thesis was to make use of data obtained from the hospitals Cancer Center. We utilized real data, which let us assess the methods we used.

5.2. FUTURE WORK

Given the exploratory character of the research for this dissertation, the findings are also instructive in terms of future research areas that are likely to provide important results. For example, because Matlab does not allow us to utilize a large number of features with ANN, a first next step would be to examine the approach more extensively using alternative programs.

The testing was primarily focused on tumor segmentation and classification accuracy rate. However, Additional testing on other well labeled data sets can demonstrate the method's accuracy in recognizing different types of tissue. Since a result, this may be highly useful for practitioners and even assist to enhance the method's diagnostic accuracy, as it is known that two types of breast tissue (the denser ones) can conceal symptoms of cancer more readily, causing them to be overlooked on scans and not apparent until later. As a result, trustworthy information on the location of such tissue, as well as a technique to further study such tissue, might provide additional diagnostic assistance.[]

REFERENCES

[1] Abdel-Maksoud E., Elmogy M., Al-Awadi R. Brain tumor segmentation based on a hybrid clustering technique // Egyptian Informatics Journal. – 2015. – T. 16. – №. 1. – C. 71-81.

[2] Alias A., Paulchamy B. Detection of Breast Cancer Using Artificial Neural Networks //International Journal of Innovative Research in Science, Engineering and Technology. – 2014. – T. 3. – №. 3. – C. 10053-10060

.

[3] Fan H., Pei J., Zhao Y. An optimized probabilistic neural network with unit hyperspherical crown mapping and adaptive kernel coverage //Neurocomputing. – 2020. – T. 373. – C. 24-34.

[4] Ghanbari S. et al. New steganalysis method using GLCM and neural network. – 2012.

[5] Sudha S., Suresh G. R., Sukanesh R. Speckle noise reduction in ultrasound images by wavelet thresholding based on weighted variance //International journal of computer theory and engineering. – 2009. – T. 1. – №. 1. – C. 7.

[6] Ahmad W. S. H. M. W. et al. Classification of infection and fluid regions in chest x-ray images //2016 International Conference on Digital Image Computing: Techniques and Applications (DICTA). – IEEE, 2016. – C. 1-5.

[7] Ali J. B. et al. Linear feature selection and classification using PNN and SFAM neural networks for a nearly online diagnosis of bearing naturally progressing degradations //Engineering Applications of Artificial Intelligence. – 2015. – T. 42. – C. 67-81.

[8] Badawy S. M. et al. Breast cancer detection with mammogram segmentation: a qualitative study //International Journal of Advanced Computer Science and Application. – 2017. – T. 8. – №. 10.

[9] Cadena L. et al. Brain’s tumor image processing using shearlet transform //Applications of Digital Image Processing XL. – International Society for Optics and Photonics, 2017. – T. 10396. – C. 103961B.

[10] Cadena L. et al. Processing medical images by new several mathematics shearlet transform. – 2016.

[11] Dalmış M. U. et al. Using deep learning to segment breast and fibroglandular tissue in MRI volumes //Medical physics. – 2017. – T. 44. – №. 2. – C. 533-546.

[12] Häuser S., Steidl G. Fast finite shearlet transform //arXiv preprint arXiv:1202.1773. – 2012.

[13] Li X., Chen L., Chen J. A visual saliency-based method for automatic lung regions extraction in chest radiographs //2017 14th International Computer Conference on Wavelet Active Media Technology and Information Processing (ICCWAMTIP). – IEEE, 2017. – C. 162-165.

[14] Andrabi Y. et al. Advances in CT imaging for urolithiasis //Indian journal of urology: IJU: journal of the Urological Society of India. – 2015. – T. 31. – №. 3. – C. 185.

[15] Candemir S., Antani S. A review on lung boundary detection in chest X-rays //International journal of computer assisted radiology and surgery. – 2019. – T. 14. – №. 4. – C. 563-576.

[16] Demirhan A., Törü M., Güler İ. Segmentation of tumor and edema along with healthy tissues of brain using wavelets and neural networks //IEEE journal of biomedical and health informatics. – 2014. – T. 19. – №. 4. – C. 1451-1458.

[17] Jaeger S. et al. Automatic tuberculosis screening using chest radiographs //IEEE transactions on medical imaging. – 2013. – T. 33. – №. 2. – C. 233-245.

[18] Cheng H. D. et al. Automated breast cancer detection and classification using ultrasound images: A survey //Pattern recognition. – 2010. – T. 43. – №. 1. – C. 299-317.

[19] et al. A computer-aided diagnosis approach for emphysema recognition in chest radiography //Medical engineering & physics. – 2013. – T. 35. – №. 1. – C. 63-73.

[20] Dou W. et al. A framework of fuzzy information fusion for the segmentation of brain tumor tissues on MR images //Image and vision Computing. – 2007. – T. 25. – №. 2. – C. 164-171.

[21] Hasan S. M. A., Ko K. Depth edge detection by image-based smoothing and morphological operations //Journal of Computational Design and Engineering. – 2016. – T. 3. – №. 3. – C. 191-197.

[22] Nandhagopal N., Gandhi K. R., Sivasubramanian R. Probabilistic neural network based brain tumor detection and classification system //Research Journal of Applied Sciences, Engineering and Technology. – 2015. – T. 10. – №. 12. – C. 1347-1357.

[23] Priya E., Srinivasan S. Automated object and image level classification of TB images using support vector neural network classifier //Biocybernetics and Biomedical Engineering. – 2016. – T. 36. – №. 4. – C. 670-678.

[24] Singh I., Sanwal K., Praveen S. Breast cancer detection using two-fold genetic evolution of neural network ensembles //2016 International Conference on Data Science and Engineering (ICDSE). – IEEE, 2016. – C. 1-6.

[25] Suzuki K. (ed.). Artificial neural networks: methodological advances and biomedical applications. – BoD–Books on Demand, 2011.

[26] Wang G. et al. Automatic brain tumor segmentation using cascaded anisotropic convolutional neural networks //International MICCAI brainlesion workshop. – Springer, Cham, 2017. – C. 178-190.

[27] Zeinali Y., Story B. A. Competitive probabilistic neural network //Integrated Computer-Aided Engineering. – 2017. – T. 24. – №. 2. – C. 105-118.

[28] Ain Q., Jaffar M. A., Choi T. S. Fuzzy anisotropic diffusion-based segmentation and texture based ensemble classification of brain tumor //applied soft computing. – 2014. – T. 21. – C. 330-340.

[29] Hamad Y. A., Simonov K. V., Naeem M. B. Detection of Brain Tumor in MRI Images, Using a Combination of Fuzzy C-Means and Thresholding //International Journal of Advanced Pervasive and Ubiquitous Computing (IJAPUC). – 2019. – T. 11. – №. 1. – C. 45-60.

[30] Kang X. et al. Diffusion properties of cortical and pericortical tissue: regional variations, reliability and methodological issues //Magnetic Resonance Imaging. – 2012. – T. 30. – №. 8. – C. 1111-1122.

[31] Leite M. et al. 3D texture-based classification applied on brain white matter lesions on MR images //Medical Imaging 2016: Computer-Aided Diagnosis. – International Society for Optics and Photonics, 2016. – T. 9785. – C. 97852N.

[32] Lo S. C. B. et al. Artificial convolution neural network for medical image pattern recognition //Neural networks. – 1995. – T. 8. – №. 7-8. – C. 1201-1214.

[33] Mathews A. B., Jeyakumar M. K. Performance Analysis of Machine Learning Based Classifiers for the Diagnosis of Lung Cancer & Comparison //Indian Journal of Public Health Research & Development. – 2018. – T. 9. – №. 12. – C. 2672-2678.

[34] Schultz T., Theisel H., Seidel H. P. Topological visualization of brain diffusion MRI data //IEEE Transactions on Visualization and Computer Graphics. – 2007. – T. 13. – №. 6. – C. 1496-1503.

[35] Canny J. A computational approach to edge detection //IEEE Transactions on pattern analysis and machine intelligence. – 1986. – №. 6. – C. 679-698.

[36] Koprivanac M. et al. Degenerative mitral valve disease-contemporary surgical approaches and repair techniques //Annals of cardiothoracic surgery. – 2017. – T. 6. – №. 1. – C. 38.

[37] Sehgal A. et al. Automatic brain tumor segmentation and extraction in MR images //2016 Conference on Advances in Signal Processing (CASP). – IEEE, 2016. – C. 104-107.

[38] Sharma P., Diwakar M., Choudhary S. Application of edge detection for brain tumor detection //International Journal of Computer Applications. – 2012. – T. 58. – №. 16.

[39] Stosic Z., Rutesic P. An improved canny edge detection algorithm for detecting brain tumors in MRI images //International Journal of Signal Processing. – 2018. – T. 3.

[40] Wang G. et al. Automatic brain tumor segmentation based on cascaded convolutional neural networks with uncertainty estimation //Frontiers in computational neuroscience. – 2019. – T. 13. – C. 56.

[41] Zanaty E. A. et al. Determination of gray matter (GM) and white matter (WM) volume in brain magnetic resonance images (MRI) //International Journal of Computer Applications. – 2012. – T. 45. – №. 3. – C. 16-22.

[42] Dalmiya S., Dasgupta A., Datta S. K. Application of wavelet-based k-means algorithm in mammogram segmentation //International Journal of Computer Applications. – 2012. – T. 52. – №. 15.

[43]   El Adoui M. et al. MRI Breast Tumor Segmentation Using Different Encoder and Decoder CNN Architectures //Computers. – 2019. – Т. 8. – №. 3. – С. 52.

[44]   Kanojia M. G., Abraham S. Breast cancer detection using RBF neural network //2016 2nd International Conference on Contemporary Computing and Informatics (IC3I). – IEEE, 2016. – С. 363-368.

[45]   Liu L. et al. Automated breast tumor detection and segmentation with a novel computational framework of whole ultrasound images //Medical & biological engineering & computing. – 2018. – Т. 56. – №. 2. – С. 183-199.

[46]   Swanson K. R., Rostomily R. C., Alvord Jr E. C. A mathematical modelling tool for predicting survival of individual patients following resection of glioblastoma: a proof of principle //British journal of cancer. – 2008. – Т. 98. – №. 1. – С. 113-119.

[47]   Types of tumours - Canadian Cancer Society // http://www.cancer.ca/en/region-selector-page/?url=%2fen%2fabout-us%2fpage-not-found%2f, last accessed: 5 /5/ 2018.

[48]   Naik, S., Doyle, S., Agner, S., Madabhushi, A., Feldman, M., & Tomaszewski, J. (2008, May). Automated gland and nuclei segmentation for grading of prostate and breast cancer histopathology. In 2008 5th IEEE International Symposium on Biomedical Imaging: From Nano to Macro (pp. 284-287). IEEE.

[49]   Zeebaree, D. Q., Haron, H., Abdulazeez, A. M., & Zebari, D. A. (2019, April). Machine learning and region growing for breast cancer segmentation. In 2019 International Conference on Advanced Science and Engineering (ICOASE) (pp. 88-93). IEEE.

[50]   Pereira, D. C., Ramos, R. P., & Do Nascimento, M. Z. (2014). Segmentation and detection of breast cancer in mammograms combining wavelet analysis and genetic algorithm. Computer methods and programs in biomedicine, 114(1), 88-101.

[51] Singh, A. K., & Gupta, B. (2015). A novel approach for breast cancer detection and segmentation in a mammogram. Procedia Computer Science, 54, 676-682.

[52] Domínguez, A. R., & Nandi, A. K. (2009). Toward breast cancer diagnosis based on automated segmentation of masses in mammograms. Pattern Recognition, 42(6), 1138-1148.

[53] Ahmed, L., Iqbal, M. M., Aldabbas, H., Khalid, S., Saleem, Y., & Saeed, S. (2020). Images data practices for semantic segmentation of breast cancer using deep neural network. Journal of Ambient Intelligence and Humanized Computing, 1-17.

[54] Wang, P., Hu, X., Li, Y., Liu, Q., & Zhu, X. (2016). Automatic cell nuclei segmentation and classification of breast cancer histopathology images. Signal Processing, 122, 1-13.

[55] Su, H., Liu, F., Xie, Y., Xing, F., Meyyappan, S., & Yang, L. (2015, April). Region segmentation in histopathological breast cancer images using deep convolutional neural network. In 2015 IEEE 12th International Symposium on Biomedical Imaging (ISBI) (pp. 55-58). IEEE.

[56] Zebari, D. A., Zeebaree, D. Q., Abdulazeez, A. M., Haron, H., & Hamed, H. N. A. (2020). Improved threshold based and trainable fully automated segmentation for breast cancer boundary and pectoral muscle in mammogram images. Ieee Access, 8, 203097-203116.

[57] Punitha, S., Amuthan, A., & Joseph, K. S. (2018). Benign and malignant breast cancer segmentation using optimized region growing technique. Future Computing and Informatics Journal, 3(2), 348-358.

[58] Benco M. et al. An advanced approach to extraction of colour texture features based on GLCM //International Journal of Advanced Robotic Systems. – 2014. – Т. 11. – №. 7. – С. 104.

[59] Chauhan A., Mittal N., Khatri S. K. Reduction of Noise of Cloud Medical Images Using Image Enhancement Technique //Advances in Interdisciplinary Engineering. – Springer, Singapore, 2019. – С. 825-835.

[60] Hien N. M., Binh N. T., Viet N. Q. Edge detection based on Fuzzy C Means in medical image processing system //2017 International Conference on System Science and Engineering (ICSSE). – IEEE, 2017. – С. 12-15.

[61] Lal S. et al. Efficient algorithm for contrast enhancement of natural images //Int. Arab J. Inf. Technol. – 2014. – Т. 11. – №. 1. – С. 95-102.

[62] Selvakumar J., Lakshmi A., Arivoli T. Brain tumor segmentation and its area calculation in brain MR images using K-mean clustering and Fuzzy C-mean algorithm //IEEE-International Conference On Advances In Engineering, Science And Management (ICAESM-2012). – IEEE, 2012. – С. 186-190.

[63] Shen D., Wu G., Suk H. I. Deep learning in medical image analysis //Annual review of biomedical engineering. – 2017. – Т. 19. – С. 221-248.

[64] Singh A. K., Gupta B. A novel approach for breast cancer detection and segmentation in a mammogram //Procedia Computer Science. – 2015. – Т. 54. – С. 676-682.

[65] Suzuki K. Overview of deep learning in medical imaging //Radiological physics and technology. – 2017. – Т. 10. – №. 3. – С. 257-273.

[66] Beale M. H., Hagan M. T., Demuth H. B. Neural network toolbox™ user’s guide //R2012a, The MathWorks, Inc., 3 Apple Hill Drive Natick, MA 01760-2098,, www. mathworks. com. – 2012.

[67] BrainWeb B. Simulated brain database //Online: http://brainweb. bic. mni. mcgill. ca/cgi/brainweb2. – 2010.

[68] Glaser J., Greene G., Hendricks S. Stereology for biological research: with a focus on neuroscience. – mbf Press, 2007.

[69] Hara H. et al. Surgical planning of Isshiki type I thyroplasty using an open-source Digital Imaging and Communication in Medicine viewer OsiriX //Acta oto-laryngologica. – 2014. – T. 134. – №. 6. – C. 620-625.

[70] Heath M. et al. Current status of the digital database for screening mammography //Digital mammography. – Springer, Dordrecht, 1998. – C. 457-460.

[71] Mohanty F. et al. Digital mammogram classification using 2D-BDWT and GLCM features with FOA-based feature selection approach //Neural Computing and Applications. – 2019. – C. 1-15.

[72] Specht D. F. Probabilistic neural networks //Neural networks. – 1990. – T. 3. – №. 1. – C. 109-118.

[73] Wu W. et al. Brain tumor detection and segmentation in a CRF (conditional random fields) framework with pixel-pairwise affinity and superpixel-level features //International journal of computer assisted radiology and surgery. – 2014. – T. 9. – №. 2. – C. 241-253.

[74] Yassine S. T. et al. A new fast brain tumor extraction method based on Nl-means and expectation maximization //2018 4th International Conference on Optimization and Applications (ICOA). – IEEE, 2018. – C. 1-5.

[75] Hamad Y. A., Simonov K., Naeem M. B. Brain's tumor edge detection on low contrast medical images //2018 1st Annual International Conference on Information and Sciences (AiCIS). – IEEE, 2018. – C. 45-50.

[76] Hamad Y. A., Simonov K., Naeem M. B. Lung Boundary Detection and Classification in Chest X-Rays Images Based on Neural Network //International Conference on Applied Computing to Support Industry: Innovation and Technology. – Springer, Cham, 2019. – C. 16.

[77] Hamad Y., Mohammed O. K. J., Simonov K. Evaluating of Tissue Germination and Growth Rate of ROI on Implants of Electron Scanning Microscopy Images //Proceedings of the 9th International Conference on Information Systems and Technologies. – 2019. – C. 1-7.

[78] Hamad Y., Simonov K., Naeem M. B. Breast Cancer Detection and Classification Using Artificial Neural Networks //2018 1st Annual International Conference on Information and Sciences (AiCIS). – IEEE, 2018. – C. 51-57.